

Inferring the Dy-N axis orientation in adsorbed DySc₂N@C₈₀ endofullerenes by linearly polarized x-ray absorption spectroscopy

Ryunosuke Sagehashi ^{1,2} Wei Chuang Lee,¹ Fupin Liu ³ Alexey A. Popov ³ Matthias Muntwiler ⁴
Bernard Delley ⁴ Peter Krüger ² and Thomas Greber ¹

¹Physik-Institut, Universität Zürich, CH-8057 Zürich, Switzerland

²Graduate School of Science and Engineering, Chiba University, 263-8522 Chiba, Japan

³Leibniz Institute of Solid State and Materials Research, D-01069 Dresden, Germany

⁴Paul Scherrer Institut, CH-5232 Villigen, Switzerland



(Received 23 February 2023; revised 12 June 2023; accepted 7 July 2023; published 4 August 2023)

Endofullerene DySc₂N@C₈₀ is a single-molecule magnet with a large magnetic anisotropy and high blocking temperature, which is promising for nanomagnetic applications. As the easy axis of magnetization coincides with the Dy-N bond direction, it is important to understand the structure of the DySc₂N unit in the fullerene cage and to control the orientation of the molecules. Here we report on the experimental determination of Dy-N axis by x-ray absorption spectroscopy (XAS) with linear polarized light at the Dy-M_{4,5} white lines. DySc₂N@C₈₀ molecules were adsorbed on a Pt(111) surface and XAS was performed as a function of temperature in the range between 35 and 300 K. The M₅/M₄ branching ratio shows a clear and reversible variation with temperature which can be explained, on the basis of a thermodynamic model, by a change of average orientation of the molecules with temperature. The XAS spectra are well reproduced by ligand field multiplet calculations. It is shown that the angle between the magnetization (Dy-N) axis and the surface plane can be directly inferred from the XAS spectra with in-plane polarization by comparison with calculated spectra. It is found that the endohedral unit is randomly oriented at room temperature but tends towards orientation parallel to the surface at low temperature, indicating a weak but non-negligible interaction between the endohedral units and the metal surface.

DOI: [10.1103/PhysRevMaterials.7.086001](https://doi.org/10.1103/PhysRevMaterials.7.086001)

I. INTRODUCTION

Single-molecule magnets (SMMs) have attracted much attention in nanomagnetism and are considered promising for future applications in high-density data storage and quantum computing system [1–3]. SMMs are characterized by a large magnetic anisotropy and a relatively high blocking temperature and they show magnetic hysteresis [4,5]. As the magnetic coupling between two SMMs is very weak, long-range order does not occur. Thus the mechanism by which the SMMs can preserve the magnetization on a macroscopic time scale is totally different from that of ferromagnets and unrelated to intermolecular exchange coupling. Instead, SMMs have large local moments and a large, uniaxial magnetic anisotropy resulting in a high potential barrier for the spin-reversal process. As a result, the thermal spin-switching time can become long enough for the observation of magnetic hysteresis [6–9].

In order to preserve the structural and magnetic properties of SMMs, it is useful to locate them inside a fullerene molecule, which is called endohedral fullerene (hereafter referred to as endofullerene). They are produced by adding metals into the graphite rods in a Krätschmer Hoffmann arc discharge reactor. By forming suitable endofullerenes, it is possible to control the charge state of the encapsulated molecule, which may have unique physical properties like luminescence and nonlinear optical response [10,11]. In particular, endofullerenes composed of three rare earth ions and one N atom inside a C₈₀ cage were found to have a strong magnetic hysteresis [6–9]. In view of applications for

devices, it is necessary to know and control the orientation of the rare-earth molecular unit in the fullerene cage. We focus on the DySc₂N@C₈₀ (*I_h*) molecule, which possesses a large magnetic hysteresis below 6 K [8,12,13].

The orientation of the endohedral plane in Dy₂ScN@C₈₀ with respect to the surface normal was determined from x-ray absorption spectroscopy (XAS) before [14,15]. In these experiments left- and right-circularly polarized x-ray absorption spectra (XAS) have been added, and compared for different x-ray incidence angles with respect to the surface. Here, we report an experimental method to infer the orientation of rare-earth-containing endofullerenes by linearly polarized x-ray absorption spectroscopy (XAS). It exploits as well a form of dichroism that depends on the orientation of the polarization of the x rays with respect to the orientation of an anisotropic electron orbital that is, in the present case, a 4f⁹ (*J_z* = ±15/2) state on the Dy atoms. The XAS of DySc₂N@C₈₀ molecules adsorbed on a Pt(111) surface were measured at the Dy M_{4,5} edge as a function of temperature in the range between 30 and 300 K. Based on ligand field multiplet calculations, it is shown that the XAS line shape strongly depends on the molecular orientation, more precisely on the angle between the light polarization vector and the Dy-N axis which is the spin-quantization axis in DySc₂N. Eventually, this makes it possible to infer the Dy-N axis orientations with respect to the surface normal from the XAS spectra. We find that the molecules are randomly oriented at room temperature, but at low temperature, there is a preferential in-plane orientation of the Dy-N axes.

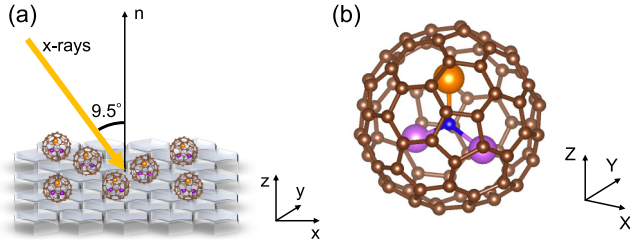


FIG. 1. (a) Scheme of the XAS experiment. The sample is $\text{DySc}_2\text{N}@C_{80}$ molecules adsorbed on a Pt(111) surface. The p-polarized x rays impinge at an angle of 9.5° with respect to the surface normal (n) which points along z in the laboratory frame. (b) Ball and stick model of $\text{DySc}_2\text{N}@C_{80}$ (orange: Dy, purple: Sc, blue: N, brown: C). The Dy-N axis points along Z in the molecular frame.

II. EXPERIMENTAL AND THEORETICAL DETAILS

A. Experiments

$\text{DySc}_2\text{N}@C_{80}$ molecules were produced by arc-discharge synthesis [13,16]. The molecules in toluene solution were printed on a Pt(111) thin film substrate [17] by using an air-brush from Harder and Steebeck [18]. Around 0.5 mL solution was sprayed for about 30 seconds on spots with a diameter of about 2 mm. After that, the sample was annealed in vacuum at 500 K for one hour in order to desorb volatile molecules including toluene. The resulting surface was characterized with x-ray photoelectron spectroscopy (XPS) [19]. Next, XAS measurements on the Dy- $M_{4,5}$ edge were performed at the Photoemission and Atomic Resolution Laboratory (PEARL) beamline at the Swiss Light Source with linear polarized x rays [20]. The total electron yield was measured with an Everhart-Thornley detector [21]. The angle between the incident x rays and the surface normal was 9.5° [see Fig. 1(a)]. During the measurements, the vacuum was better than 1×10^{-10} mbar and the temperature of the sample was changed via a liquid helium cryostat [20].

B. Calculations

XAS calculations were performed on the $M_{4,5}$ edge of the Dy atom in the DySc_2N molecule with the “multiX” ligand field multiplet program [22]. The energy levels and oscillator strengths of core-valence excitations are calculated with the single ion multiplet Hamiltonian $\mathcal{H}_{\text{mult}}$ composed of Coulomb interaction, spin-orbit coupling, and crystal field. Also, these parameters are defined within point charge model, so $\mathcal{H}_{\text{mult}}$ is given by

$$\mathcal{H}_{\text{mult}} = \sum_{i,j(<i)}^n \frac{e^2}{|\mathbf{r}_i - \mathbf{r}_j|} + \sum_{i=1}^n \epsilon_i + \sum_{i=1}^n \sum_{m=1}^N \frac{-eQ_m}{|\mathbf{r}_i - \mathbf{R}_m|}. \quad (1)$$

On the right-hand side of this equation, the first term is the Coulomb interaction of n electrons in the open shells of the target atom. The second one is a single electron operator including the effect of the kinetic energy and spin-orbit coupling, and ϵ_i are the eigenvalues of the Dirac equation. The third one is the crystal field formed by N point charges (Q_m) at position \mathbf{R}_m from the target atom. In this case, we considered

TABLE I. Atomic positions and charges of DySc_2N around Dy^{3+} ion used in the calculation. The data is taken from Ref. [23].

| atom | X (Å) | Y (Å) | Z (Å) | charge (e) |
|-------|--------|-------|--------|------------|
| N | 0.000 | 0.000 | -2.173 | -1.705 |
| Sc(1) | -1.701 | 0.000 | -3.154 | +1.724 |
| Sc(2) | 1.698 | 0.000 | -3.155 | +1.719 |

the $M_{4,5}$ edge absorption process, so the electronic transition in the Dy^{3+} ion is $3d^{10}4f^9 \rightarrow 3d^94f^{10}$.

Table I lists the positions and charges of atoms in the molecule. (The Dy atom is located on the origin.) XAS calculation was performed with linear polarized light along one of the three molecular axes [X, Y, Z in Fig. 1(b)]. Various parameter values of $\mathcal{H}_{\text{mult}}$ were rescaled by fit to the experimental XAS spectra. (Details are given in the Supplemental Materials [19].)

III. RESULTS AND DISCUSSION

In the measurements, 170 x-ray-induced electron yield spectra on the Dy- $M_{4,5}$ edge that correspond to $3d^94f^{10}$ final state multiplets at different temperatures were recorded [19]. Figure 2(a) displays an XAS spectrum obtained at room temperature, where the scan took about two minutes. The background shown as a dashed line in Fig. 2(a) is determined by fitting a base line with a third-order polynomial function with 4 parameters and was used for the background removal as described in Ref. [21]. The background removal procedure was normalization of the XAS spectra by their baseline, and subtraction of 1. In these spectra, the main M_5 peak is at 1292.6 eV photon energy. After background removal, we find a significant variation of the spectral weight of the M_5 edge W_{M_5} defined as $\frac{\int I_{M_5} dE}{\int I_{M_4+M_5} dE}$. Figure 2(b) shows the values of the weight as a function of temperature. In this figure, $W_{M_5}(T)$ decreases with temperature from 82% to 79%. As we will argue in the following, this is the fingerprint of different Dy-N axis angle distributions with respect to the surface normal for different temperatures. $W_{M_5}(T)$ may be fitted with a thermodynamic model that mimics the freezing of molecular degrees of freedom of an endofullerene molecule at low temperature [19,24]. The black solid line in Fig. 2(b) was obtained by fitting the data to a two-state model function, which is

$$W_{M_5}(T) = W_0 + \Delta W \frac{(1 + N_1) \exp(-\Delta E/k_B T)}{1 + N_1 \exp(-\Delta E/k_B T)}, \quad (2)$$

where W_0 is the weight for $T \rightarrow 0$, and $\Delta W = W_\infty - W_0$, with the weight W_∞ for $T \rightarrow \infty$. N_1 is the degeneracy of the excited level that is lying ΔE above the degenerate ground state. As a result, the fit indicates an excitation energy $\Delta E/k_B$ of 225 K with $N_1 = 6$ endohedral orientations in the excited state. Some temperature dependence of W_{M_5} is expected from the thermal excitation from the ground state Kramers doublet ($J_z = \pm 15/2$) to higher levels ($J_z = \pm 13/2$, etc.) since the M_5/M_4 branching ratio depends on J_z . We have calculated $W_{M_5}(T)$ induced by this electronic effect using a ligand field that reproduces the first excitation energy

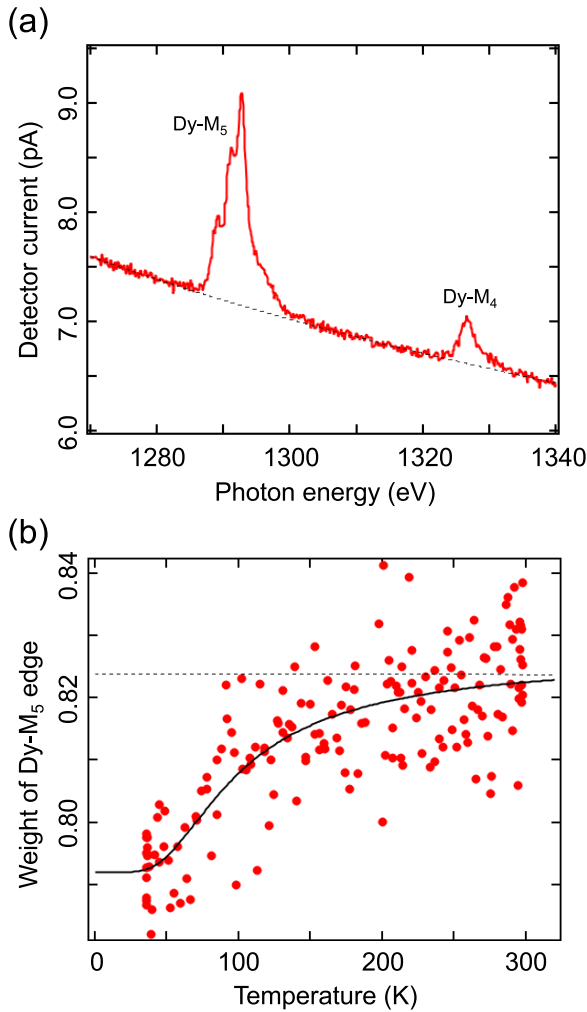


FIG. 2. (a) XAS spectrum on the Dy- $M_{4,5}$ edge at room temperature. The dashed line is the background baseline. (b) Spectral weight of the Dy- M_5 edge ($\frac{\int I_{M_5} dE}{\int I_{M_4+M_5} dE}$). The solid line is a fit of a thermodynamic model [Eq. (2)]. The dashed line is the expectation from a theory with a $J_z = \pm 15/2 \rightarrow \pm 13/2$ splitting of 47 meV (obtained from Fig. S7 in the Supplemental Materials [19]).

of 47 meV [23] and assuming a random orientation of the quantization axis (Dy-N). (Note that the thermal population of all excited levels is included in the multiX code. See the Supplemental Materials [19] for more details.) The result is shown as a dashed line in Fig. 2(b). The average W_{M_5} value agrees well with the experiment, indicating that the assumption of near-random orientation of the quantization axis is justified. However, compared to the experimental data points, the temperature dependence of the theoretical $W_{M_5}(T)$ is much weaker and of the opposite sign (see Fig. S7 in the Supplemental Materials [19]), which shows that the observed temperature effect cannot be explained by a magnetic excitation. More likely, the observed $W_{M_5}(T)$ reflects the onset of endohedral rotation [24–27] and indicates that the surface must influence the endohedral cluster orientation.

In order to quantify the temperature effect in the XAS spectra, we also calculated XAS spectra on Dy atoms of DySc_2N

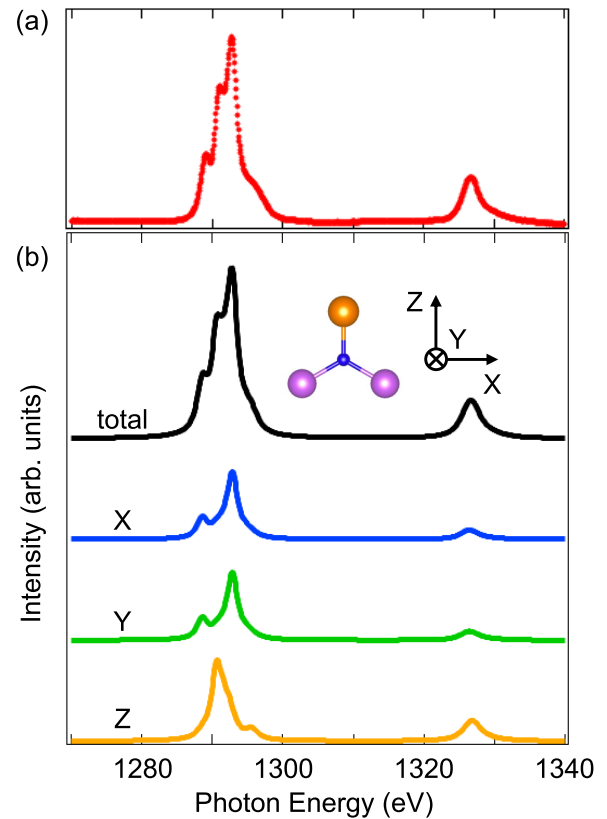


FIG. 3. Comparison between experiment and theory. (a) Average of all experimental spectra after background removal. (b) Calculated XAS spectra on the $M_{4,5}$ edges of a Dy atom for linear polarized x rays along X (blue), Y (green), and Z (yellow). The black line is the sum of I_X , I_Y , and I_Z . The inset depicts the DySc_2N endohedral unit and the molecular reference frame. The close resemblance of the black line and the experiment indicates random orientation of the Dy-N axes.

endohedral units for different orientations of the x-ray polarization vector with respect to the Dy-N or Z axis in the molecular frame of reference. As it was shown for circularly polarized light, the x rays are very sensitive to the angle between the incoming light and the Dy-N axis [6,15] and theory may predict the endohedral orientation [6]. For the present case, this has been obtained by ligand field calculations that confirm a $J_z = \pm 15/2$ ground state for the Dy^{3+} ions and a high magnetic excitation energy of 47 meV of the $J_z = \pm 13/2$ states [23]. Figure 3 shows the average experimental spectrum after background subtraction and calculated XAS spectra. The two calculated spectra with light polarization along X and Y are very similar and confirm the picture that the N^{3-} ion dominates the ligand field. The two Sc^{3+} ions are more distant to the Dy atom and also sum up to a contribution along the Dy-N axis. The average experimental spectrum [Fig. 3(a)] resembles the sum of the calculated spectra $I_X + I_Y + I_Z$. This indicates that the Dy-N axes are distributed almost evenly in the laboratory frame. In the following, we searched for the optimal linear combination of the calculated spectra that fits the experiments. Since $I_X \approx I_Y$ in Fig. 3(b), we set $I_X = I_Y$ and describe the experimental spectra as a linear combination

of I_Z and I_X :

$$I_{\text{exp}} = A (\kappa I_Z + (1 - \kappa) I_X), \quad (3)$$

where A is the proportionality factor between experiment and theory and κ is a directional parameter. κ is $1/3$ for the isotropic Dy-N or Z-axis distribution in the laboratory frame, and $\kappa = 1/2$ is expected for a distribution where the Z axes are distributed uniformly in the surface plane perpendicular to the incoming light. For the average spectrum in Fig. 3(b), we find $\kappa = 0.336 \pm 0.003$ which confirms the guess by naked eye that it is close to $1/3$.

The directional parameter κ can be translated into an angular scale. Applying the Euler angles for the description of the rotation about the Z axes, we find $\kappa = (1 - \cos^2 \beta)/2$, where β is the angle between the Z axis and the wave vector of the incoming light, which in the present case, is close to the surface normal. This relation holds under the common assumption that the in-plane (azimuthal) orientation of adsorbed molecules is random [28] (see Supplemental Materials [19] for details). For the isotropic case, β corresponds to the magic angle of 54.74° . For the present experimental geometry, a β angle larger than the magic angle means that the Z axes are preferentially oriented in the surface plane.

In order to estimate the orientation of DySc₂N clusters at different temperatures, we fitted the β values to the experimental spectra. For this purpose, five subsequent spectra were added in order to obtain better signal-to-noise ratios, and furthermore, the small drift of the photon energy during the measurement was corrected [19]. Figure 4 shows a fit for 300 K and for 35 K that yield significantly different β values of $(54.58 \pm 0.19)^\circ$ and $(56.23 \pm 0.20)^\circ$, respectively. This indicates that a difference in β below 1.5° may be detected with the present accuracy of the experiment. The change of β with temperature is statistically significant as shown in Fig. S4 (Supplemental Materials [19]). The second Euler angles β of all spectral groups are shown in Fig. 5. While at room temperature β is close to the magic angle, it increases at lower temperatures. This confirms interaction of the endohedral cluster across the C₈₀ carbon shell and indicates that the Dy-N axes tend to align parallel to the surface. Such an endohedral alignment tendency was reported in previous studies [6,29–33]. The transition temperature scale of 225 K is a measure for the energy difference between different endohedral configurations, where higher ordering is expected at lower temperatures. The interaction is electrostatic in nature [34] and the ordering mechanism must involve the screening of the endohedral charge by the substrate electrons. For spherical C₈₀ with a constant adsorption height, the screening is better if the endohedral ions are aligned parallel to the metal surface on which they are adsorbed.

The present result of observed increased alignment at low temperature is a benchmark for the attainable accuracy for the quantification of the effect in ensemble samples. Given the sample preparation with an airbrush and some unwanted Si contamination, we consider this result to be remarkable. The solid black line in Fig. 5 depicts the scaled model that was used for the description of the $W_{M_5}(T)$ behavior [Fig. 2(b)], together with the 90% prediction bands that indicate the effect

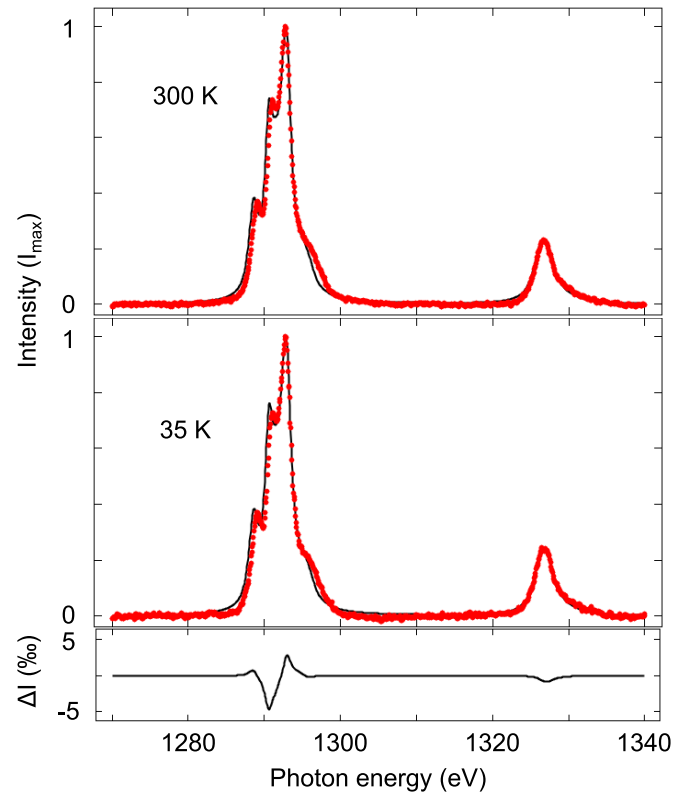


FIG. 4. Experimental XAS spectral groups (red dots) fitted to I_Z and I_X (black lines). Top panels: 300 K and 35 K. Bottom panel: difference between the fits at room temperature and low temperature.

to be statistically significant. The β values from the fits predict $W_{M_5} = 82.3\%$ for the magic angle and 82.0% for $\beta = 56.2^\circ$ [19]. W_{M_5} at the magic angle corresponds well to the experimental value at room temperature. Although the change in

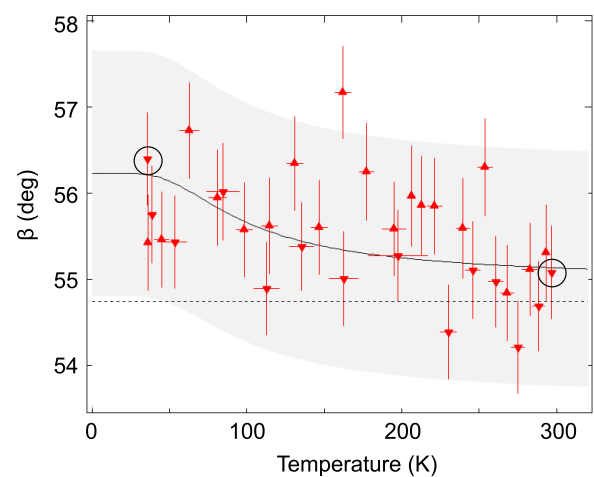


FIG. 5. Temperature dependence of the second Euler angle β of the Dy-N axes distribution. β values as a function of temperature for groups of 5 subsequent spectra. (▼ cooling, ▲ heating). The circles indicate the spectra shown in Fig. 4. The black solid line with the 90% prediction intervals (light gray) represents the model in Fig. 2(b), now fitted to the second Euler angles β .

W_{M_5} in going to low temperature of 0.3% from the fits is smaller than the corresponding value from the experiment (3%), we conjecture that W_{M_5} is a useful fingerprint for the detection of endohedral reorientation and for the extraction of thermodynamic data. Given the systematic uncertainties for the absolute determination of W_{M_5} from the experiment [21], the rotation angles should be obtained from the κ values of the fits rather than the experimentally determined W_{M_5} values.

IV. CONCLUSIONS

Experimentally, we obtained distinct XAS spectra on the Dy- $M_{4,5}$ edge in adsorbed DySc₂N@C₈₀ molecules at different temperatures, where the weight of the M₅ edge decreases with temperature. Comparison of the experiments with calculated XAS spectra suggests a conformation change of DySc₂N

molecules as a function of temperature, where the endohedral units in DySc₂N@C₈₀ tend to arrange towards a parallel orientation on the investigated Pt(111) substrate.

ACKNOWLEDGMENTS

This work is supported by the Swiss National Science Foundation (Grant No. 201086). R.S. acknowledges support by Chiba University Open Recruitment for International Exchange Program and the Japan Science and Technology Agency (JST) with the establishment of University fellowships towards the creation of science technology innovation (Grant No. JP-MJFS2107). The XAS measurements were performed at the PEARL beamline of the Swiss Light Source, Paul Scherrer Institut, Villigen. A.A.P. acknowledges Deutsche Forschungsgemeinschaft (Grant No. PO 1602/8-1).

-
- [1] M. N. Leuenberger and D. Loss, *Nature (London)* **410**, 789 (2001).
- [2] L. Bogani and W. Wernsdorfer, *Nat. Mater.* **7**, 179 (2008).
- [3] F. Troiani and M. Affronte, *Chem. Soc. Rev.* **40**, 3119 (2011).
- [4] R. Sessoli, D. Gatteschi, A. Caneschi, and M. A. Novak, *Nature (London)* **365**, 141 (1993).
- [5] D. Gatteschi, R. Sessoli, and J. Villiaín, *Molecular Nanomagnets* (Oxford University Press, New York, 2006).
- [6] R. Westerström, J. Dreiser, C. Piamonteze, M. Muntwiler, S. Weyeneth, K. Krämer, S. X. Liu, S. Decurtins, A. A. Popov, S. Yang, L. Dunsch, and T. Greber, *Phys. Rev. B* **89**, 060406(R) (2014).
- [7] A. Kostanyan, C. Schlesier, R. Westerström, J. Dreiser, F. Fritz, B. Büchner, A. A. Popov, C. Piamonteze, and T. Greber, *Phys. Rev. B* **103**, 014404 (2021).
- [8] R. Nakanishi, J. Satoh, K. Katoh, H. Zhang, B. K. Breedlove, M. Nishijima, Y. Nakanishi, H. Omachi, H. Shinohara, and M. Yamashita, *J. Am. Chem. Soc.* **140**, 10955 (2018).
- [9] S. Ito, R. Nakanishi, K. Katoh, B. K. Breedlove, T. Sato, Z. Y. Li, Y. Horii, M. Wakizaka, and M. Yamashita, *Dalton Trans.* **51**, 6339 (2022).
- [10] I. V. Mikheev, M. M. Sozarukova, E. V. Proskurnina, I. E. Kareev, and M. A. Proskurnin, *Molecules* **25**, 2506 (2020).
- [11] A. K. Srivastava, A. Kumar, and N. Misra, *Chem. Phys. Lett.* **682**, 20 (2017).
- [12] R. Westerström, J. Dreiser, C. Piamonteze, M. Muntwiler, S. Weyeneth, H. Brune, S. Rusponi, F. Nolting, A. A. Popov, S. Yang, L. Dunsch, and T. Greber, *J. Am. Chem. Soc.* **134**, 9840 (2012).
- [13] D. S. Krylov, F. Liu, A. Brandenburg, L. Spree, V. Bon, S. Kaskel, A. U. B. Wolter, B. Büchner, S. M. Avdoshenko, and A. A. Popov, *Phys. Chem. Chem. Phys.* **20**, 11656 (2018).
- [14] R. Westerström, A. C. Uldry, R. Stania, J. Dreiser, C. Piamonteze, M. Muntwiler, F. Matsui, S. Rusponi, H. Brune, S. Yang, A. Popov, B. Büchner, B. Delley, and T. Greber, *Phys. Rev. Lett.* **114**, 087201 (2015).
- [15] T. Greber, A. P. Seitsonen, A. Hemmi, J. Dreiser, R. Stania, F. Matsui, M. Muntwiler, A. A. Popov, and R. Westerström, *Phys. Rev. Mater.* **3**, 014409 (2019).
- [16] C. Schlesier, F. Liu, V. Dubrovín, L. Spree, B. Büchner, S. M. Avdoshenko, and A. A. Popov, *Nanoscale* **11**, 13139 (2019).
- [17] A. Hemmi, H. Cun, S. Brems, C. Huyghebaert, and T. Greber, *J. Phys. Mater.* **4**, 044012 (2021).
- [18] A. Kostanyan, C₈₀ endohedral fullerenes: Rearranging atoms in a magnetic field and exploring the interplay of their spins with subkelvin magnetometry and X-rays, Ph.D. thesis, Univ. of Zürich, 2018.
- [19] See Supplemental Materials at <http://link.aps.org/supplemental/10.1103/PhysRevMaterials.7.086001> for sample preparation, obtained XAS data, the calculation conditions, and the idea of determination of the Dy-N bond orientation.
- [20] M. Muntwiler, J. Zhang, R. Stania, F. Matsui, P. Oberta, U. Flechsig, L. Patthey, C. Quitmann, T. Glatzel, R. Widmer, E. Meyer, T. A. Jung, P. Aebi, R. Fasel, and T. Greber, *J. Synchrotron Radiat.* **24**, 354 (2017).
- [21] W. C. Lee, R. Sagehashi, Y. Zhang, A. A. Popov, M. Muntwiler, and T. Greber, *J. Vac. Sci. Technol. A* **40**, 053205 (2022).
- [22] A. C. Uldry, F. Vernay, and B. Delley, *Phys. Rev. B* **85**, 125133 (2012).
- [23] Y. Zhang, D. Krylov, M. Rosenkranz, S. Schiemenz, and A. A. Popov, *Chem. Sci.* **6**, 2328 (2015).
- [24] R. Stania, A. P. Seitsonen, H. Jung, D. Kunhardt, B. Büchner, A. A. Popov, M. Muntwiler, and T. Greber, [arXiv:2205.07342](https://arxiv.org/abs/2205.07342) (2022).
- [25] K. R. Górný, C. H. Pennington, J. A. Martindale, J. P. Phillips, S. Stevenson, I. Heinmaa, and R. Stern, [arXiv:cond-mat/0604365v1](https://arxiv.org/abs/cond-mat/0604365v1) (2006).
- [26] Y. Zhang, D. Krylov, S. Schiemenz, M. Rosenkranz, R. Westerström, J. Dreiser, T. Greber, B. Büchner, and A. A. Popov, *Nanoscale* **6**, 11431 (2014).
- [27] A. Kostanyan, R. Westerström, Y. Zhang, D. Kunhardt, R. Stania, B. Büchner, A. A. Popov, and T. Greber, *Phys. Rev. Lett.* **119**, 237202 (2017).
- [28] S. Kera, H. Yamane, H. Fukagawa, T. Hanatani, K. K. Okudaira, K. Seki, and N. Ueno, *J. Electron Spectrosc. Relat. Phenom.* **156-158**, 135 (2007).

- [29] M. Treier, P. Ruffieux, R. Fasel, F. Nolting, S. Yang, L. Dunsch, and T. Greber, *Phys. Rev. B* **80**, 081403(R) (2009).
- [30] S. M. Avdoshenko, F. Fritz, C. Schlesier, A. Kostanyan, J. Dreiser, M. Luysberg, A. A. Popov, C. Meyer, and R. Westerström, *Nanoscale* **10**, 18153 (2018).
- [31] D. S. Krylov, S. Schimmel, V. Dubrovin, F. Liu, T. T. N. Nguyen, L. Spree, C. H. Chen, G. Velkos, C. Bulbucan, R. Westerström, M. Studniarek, J. Dreiser, C. Hess, B. Büchner, S. M. Avdoshenko, and A. A. Popov, *Angew. Chem. Int. Ed.* **59**, 5756 (2020).
- [32] C. H. Chen, L. Spree, E. Koutsouflakis, D. S. Krylov, F. Liu, A. Brandenburg, G. Velkos, S. Schimmel, S. M. Avdoshenko, A. Fedorov, E. Weschke, F. Choueikani, P. Ohresser, J. Dreiser, B. Büchner, and A. A. Popov, *Adv. Sci.* **8**, 2000777 (2021).
- [33] V. Dubrovin and S. M. Avdoshenko, *J. Comput. Chem.* **43**, 1614 (2022).
- [34] R. Stania, A. P. Seitsonen, D. Kunhardt, B. Büchner, A. A. Popov, M. Muntwiler, and T. Greber, *J. Phys. Chem. Lett.* **9**, 3586 (2018).